INTERNATIONAL JOURNAL OF INTEGRATED ENGINEERING
ISSN: 2229-838X e-ISSN: 2600-7916

IJIE

Vol. 17 No. 6 (2025) 280-291
https://publisher.uthm.edu.my/ojs/index.php/ijie

# Microstrip Patch Antenna Design for Natural Rubber Permittivity Detection

**Muhammad Sazlan Abdul Kadar[1], Siti Zarina Mohd Muji[1]*, Fatin Hamimah Ikhsan[1], Ariffuddin Joret[1],Yee See Khee[1], Fauziahanim Che Seman[1], Ruzairi Abdul Rahim[2], Nadras Othman[3]**

[1] *Faculty of Electric and Electronic Engineering,*
*Universiti Tun Hussein Onn Malaysia (UTHM), 86400 Parit Raja, Batu Pahat, Johor, MALAYSIA*
[2] *Faculty of Electrical Engineering,*
*Universiti Teknologi Malaysia (UTM), 81310 Skudai, Johor, MALAYSIA*
[3] *School of Materials & Mineral Resources Engineering,*
*Universiti Sains Malaysia, Nibong Tebal, 14300 Seberang Prai Selatan, Pulau Pinang, MALAYSIA*

*Corresponding Author: szarina@uthm.edu.my
DOI: https://doi.org/10.30880/ijie.2025.17.06.023

**Article Info**

Received: 30 May 2025
Accepted: 13 September 2025
Available online: 30 December 2025

**Keywords**

Microstrip patch antenna, natural rubber, permittivity detection, dielectric sensing, vector network analyzer (VNA)

**Abstract**

This paper presents a simulation-based analysis on a rectangular microstrip patch antenna sensor capable of detecting changes in natural rubber (NR) permittivity using CST Microwave Studio. In this work, the patch antenna sensor was designed with a gap distance of 1.0 mm, 1.5 mm, and 2.0 mm between the patch and the feeder, which affects the resonance characteristics of the antenna and enhances the interaction between its radiated waves and the NR, which is the Material Under Test (MUT). As the dielectric properties were disposed of between 2.7 to 4.8 according to the experimental observable (using vector network analyzer (VNA) and dielectric probe) for NR samples in simulation model. This could be helpful in designing to see how the gap distance affects the resonant frequency shift of the antenna, return loss, and sensitivity. The 2.0 mm gap configuration in this study has the highest sensitivity of -0.0072 GHz/ε with the linear measurement rate of 0.9979, which is more sensitive to the changes of dielectric. Therefore, these results verify the capability of the microstrip patch antenna sensor for precise and dependable permittivity detection in agriculture applications.

## 1. Introduction

The microstrip patch antenna (MPA) sensor has emerged as a promising choice for advanced sensing systems because of its small size, low cost, and its high sensitivity concerning dielectric changes [1]. These advantages include compact size, low fabrication cost, ease of integration with wireless systems, high sensitivity, and the ability to operate at microwave frequencies, making them suitable for various industrial and scientific application [2]. Researchers have explored different microstrip antenna configurations for sensing applications, such as resonant frequency-based sensors [3, 4] , slot-loaded antennas [5, 6] and metamaterial-inspired designs [7, 8], which have demonstrated excellent performance in detecting variations in dielectric properties of materials. Dielectric property measurement plays a crucial role in many fields, including material characterization, biomedical applications, agriculture, and industrial quality control [1, 9, 10]. In particular, the permittivity detection of natural rubber (NR) is essential for quality assessment in the rubber industry, as variations in dielectric properties can indicate changes in composition, moisture content, or contamination levels [11]. Several

dielectric measurement techniques, including resonant cavity perturbation, waveguide-based sensors, and open-ended coaxial probes, have been explored [12]. However, these methods often involve complex fabrication processes, expensive measurement equipment, and limited adaptability to industrial settings [13].

Additionally, other research has explored the use of microstrip patch antennas integrated with Defected Ground Structures (DGS) for sensing applications in rubber-based materials. For example, a study in [14] investigated a triple-frequency rectangular patch antenna designed for moisture content detection in Hevea latex rubber. The antenna operated at 2.8 GHz, 7.8 GHz, and 8.8 GHz and showed excellent return loss characteristics, demonstrating sensitivity to changes in moisture through shifts in dielectric properties. The integration of DGS helped minimize spurious feed radiation and enabled better coupling between the sensor and the material under test (MUT). These findings reinforce the versatility of microstrip patch antenna configurations in rubber characterization applications, and support the approach adopted in this paper to explore dielectric sensing of natural rubber using electromagnetic field interactions. Prior research has also emphasized the use of microwave-based sensing techniques to detect moisture content in rubber latex. In [15] demonstrated an optimized microstrip sensor design for measuring moisture in natural rubber latex, achieving accurate results using microwave characterization methods. Similarly, a study conducted in [16] conducted a comparative analysis of different methods for detecting resonant frequency shifts in microstrip patch antennas loaded with Hevea latex, further validating the suitability of this technique for dielectric sensing in rubber materials. Recent developments have further improved sensing accuracy and sensitivity in latex-based applications. The approach in [17] proposed calibration equations based on complex permittivity measurements of Hevea latex at 5 GHz, yielding minimal mean error for dry rubber content estimation. Moreover, a modified SMA-connector sensor presented in [18] enabled accurate measurement of real and imaginary dielectric constants in natural latex across a 0.5–4 GHz frequency range, highlighting strong correlation with moisture content.

Building upon these prior advancements, this study presents a simplified rectangular microstrip patch antenna sensor specifically designed to detect changes in the permittivity of natural rubber (NR). Sensing is based on the interaction between the NR, or material under test, and the radiated waves of the antenna. The resonant frequency, return loss, and impedance matching of the antenna are affected by changes in the dielectric constant of the material under test (MUT). In this paper the permittivity change sensor of the NR as the microstrip antenna was simulated and modeled by CST Microwave Studio, which is an electromagnetic simulator commonly adopted in the industry and based on the finite integration technique [19].

In this study, we analyze the impact of changing the gap between the patch and ground plane of a rectangular microstrip antenna to 1.0 mm, 1.5 mm, and 2.0 mm to assess the wave propagation behaviour of the antenna, resonant frequency shift, and return loss of the antenna. These values of gaps were chosen to match the real spacing of the sensor along the conveyor, between 1 mm and 3 mm. These were chosen to analyze the effect of spacing variation on impedance matching of the antenna, wave propagation, and frequency shift of the resonant frequency. Gap is a very important parameter that will determine the intensity of interaction between radiated waves and NR, and hence the accuracy and efficiency of the sensor. In this simulation the dielectric properties of the NR samples were determined as between 2.7 and 4.8, which have been measured experimentally using a vector network analyzer and a N1500A dielectric probe. The suggested microstrip patch antenna sensor is an inexpensive, easy, and dependable method for permittivity sensing in NR applications with high industrial and material characterization insights.

## 2. Modelling and Method

This section outlines the experimental setup for dielectric property measurement of natural rubber (NR) and the CST-based simulation workflow used to optimize a rectangular microstrip patch antenna sensor for enhanced sensitivity and accuracy. To achieve this, dielectric measurements of NR were conducted using the setup illustrated in Fig. 1, and the extracted data were subsequently employed in CST Microwave Studio to validate and refine the antenna design for reliable permittivity detection. The NR sample was placed on a laboratory jack and secured with a sample holder to ensure stable positioning and consistent contact with the N1501A dielectric probe kit, which was connected to a vector network analyzer (VNA) via a coaxial cable for precise acquisition of reflection coefficient data. The VNA was interfaced with a Windows-based PC through a GPIB cable to enable automated data transfer and storage. During measurement, dielectric properties were extracted from the recorded S-parameter data, while fine vertical adjustments of the sample height were made using the laboratory jack to maintain proper probe–sample contact and minimize measurement errors. All measurements were displayed in real time on the VNA and simultaneously recorded on the PC for subsequent analysis and interpretation.

Int. Journal of Integrated Engineering Vol. 17 No. 6 (2025) p. 280-291

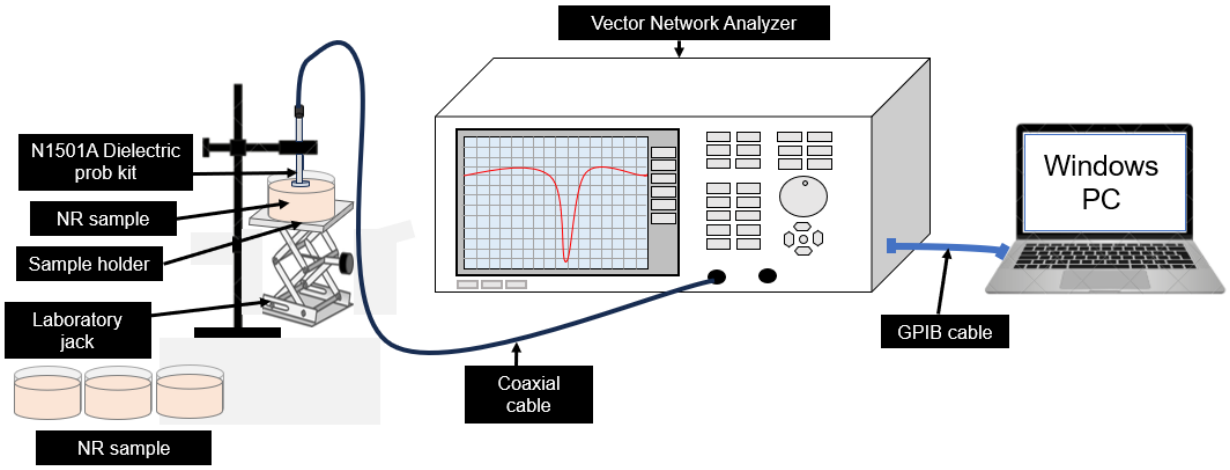


**Fig. 1** *Experimental setup for measuring the dielectric of NR*

Then, the sensor was designed and simulated using CST Microwave Studio, with mechanism of sensing based on the interaction with the radiated electromagnetic fields and the Material Under Test (MUT). This interaction changes the effective system's permittivity, which causes changes in the resonant frequency and return loss, $S_{11}$ of the antenna. The microstrip patch antenna structure consists of a rectangular patch, feedline, ground plane, and on a dielectric substrate, each optimized for maximum sensitivity to permittivity changes in NR materials. Simulations were carried out using CST Microwave Studio's Frequency Domain Solver for examining the scattering parameters (S-parameters) and electromagnetic field distribution. NR were deposited above the sensor, the fringing fields extending from the patch interacted with the MUT, altering the antenna's effective permittivity and resonant properties. This was in measurable resonant frequency and return loss, $S_{11}$ that were tested to analyze the sensitivity and detecting capability of the sensor. The effect of different gap configurations on the antenna performance were analyzed, with emphasis on important parameters like resonant frequency shift, return loss, $S_{11}$ and sensitivity.

For comprehension of the sensing mechanism of the rectangular microstrip patch antenna sensor, comprehension of how fringing fields contribute to the coupling between the antenna and the material under test (MUT) is required. In microstrip patch antennas, fringing fields are electromagnetic fields that extend beyond the patch boundary, hence into the ambient medium. These applications are highly sensitive to changes in the material dielectric properties placed close to the antenna and are therefore well adapted to application in permittivity sensing. The structure employed in this study, as illustrated in Fig. 2, was chosen because of its ease of design and the fact that it is one of the simplest models to employ when one is designing a rectangular microstrip patch antenna [20].

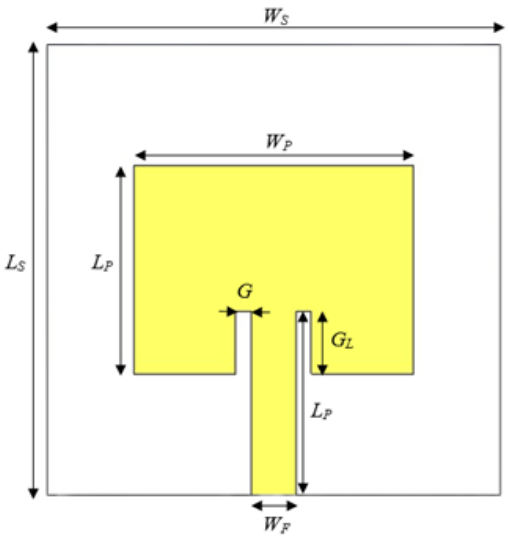


**(a)**

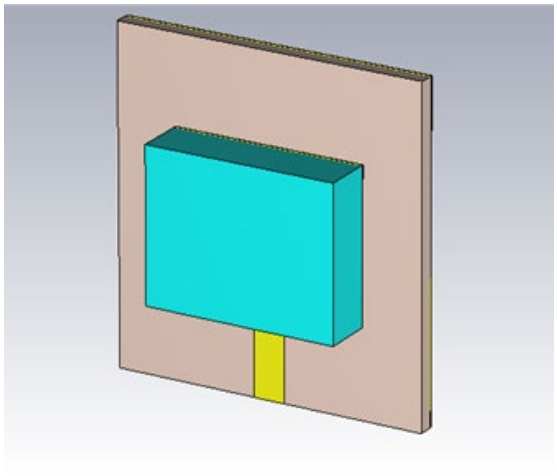

**(b)**

**Fig. 2** *Microstrip patch antenna model with MUT (a) Dimension; (b) 3D-view*

Furthermore, the dielectric substrate used in this structure is FR4 with a height of 1.6 mm and a dielectric constant of $\varepsilon_r$ = 4.3. Thus, the proposed antenna design is guided by these equations (1)-(5) [21]. In the calculation step, the width of the patch should be determined from the following relationship [22][23]:

Step 1: Size of width, $W_P$

$$W_P = \frac{C}{2f_r}\sqrt{\frac{2}{\varepsilon_r + 1}} = \frac{3 \times 10^8}{2 \times 5 \times 10^9}\sqrt{\frac{2}{4.3 + 1}} = 18.4\, mm \tag{1}$$

where $W_P$ represents the patch width, $\varepsilon_r$ = denotes the substrate's relative permittivity, $f_r$= desired resonant frequency, c is referring to the speed of light.

To determine the length of the patch, the effective dielectric constant, $\varepsilon_{reff}$ of substrate must be calculated. It is defined by the step 2 [24][25].

Step 2: Estimate of effective dielectric constant, $\varepsilon_{reff}$

$$\varepsilon_{reff} = \frac{\varepsilon_r + 1}{2} + \frac{\varepsilon_r - 1}{2}\left[1 + 12\frac{h}{W_P}\right]^{-\frac{1}{2}} = \frac{4.3 + 1}{2} + \frac{4.3 - 1}{2}\left[1 + 12\frac{1.6}{18.4}\right]^{-\frac{1}{2}} = 3.8 \tag{2}$$

where $\varepsilon_r$ is the relative permittivity of the substrate, $h$ is the substrate thickness, and $W_p$ is the width of the patch. As the dielectric properties of the MUT change, the effective dielectric constant $\varepsilon_{reff}$ is modified, leading to measurable shifts in the antenna's response.

Upon calculating effective dielectric constant, $\varepsilon_{reff}$, the effective length, $L_{eff}$ of patch should be determine by step 3 [26].

Step 3: Estimate of Effective length, $L_{eff}$

$$L_{eff} = \frac{C}{2f_r\sqrt{\varepsilon_{reff}}} = \frac{3 \times 10^8}{2 \times 5 \times 10^9\sqrt{3.8}} = 15.38\, mm \tag{3}$$

The extension of length ΔL of the microstrip antenna due to the fringing field's effect can be determined in step 4 [27][28].

Int. Journal of Integrated Engineering Vol. 17 No. 6 (2025) p. 280-291

Step 4: Estimate of the extent in length, ΔL

$$\Delta L = 0.412h \frac{\varepsilon_{reff} + 0.3(\frac{W_P}{h} + 0.264)}{\varepsilon_{reff} - 0.258(\frac{W_P}{h} + 0.8)} = 0.412(1.6)\frac{3.8 + 0.3\left(\frac{18.4}{1.6} + 0.264\right)}{3.8 - 0.258\left(\frac{18.4}{1.6} + 0.8\right)} = 0.73\, mm \quad (4)$$

After considering fringing field's effect, the final effective length of the patch antenna can be calculated in step 5.

Step 5: Estimate of actual length of patch, $L_P$

$$L_P = L_{eff} - 2\Delta L = 15.38 - (2)(0.73) = 13.92 \text{ mm} \quad (5)$$

The geometric dimension of the antenna is calculated using MATLAB and simulations made for this antenna have been performed using CST Microwave Studio. After initial simulation, the software parameter sweep was used to optimize the microstrip patch antenna (MPA) design. In this project, once the size of the radiating element is determined, the size of the substrate is assumed to be greater than the radiating element and was further adjusted by tuning its dimensions. Besides, to achieve better impedance matching between the feed line and the radiating patch, the inset feed gap method is adopted, thereby increasing the return loss at the resonant frequency [29]. The width of the feed line for this antenna was fixed at 3.05 mm to implement 50 Ohm characteristic impedance of the SMA connector. As a result, the basic antenna's dimensions have been tuned till the working frequency is resonant at 5 GHz. The antenna dimensions, provided in Table 1, define the structural parameters essential for performance optimization.

**Table 1** *Sensor parameter settings in CST microwave studio*

| Parameter | Value |
|---|---|
| Patch Length, $L_P$ | 13.89mm |
| Patch Width, $W_P$ | 18.5mm |
| Gap Length, $G_L$ | 4.19mm |
| Gap Width, G | 1mm, 1.5mm and 2mm |
| Feed Width, $W_F$ | 3.05mm |
| Feed Length, $L_F$ | 12.25mm |
| Substrate Length, $L_S$ | 30mm |
| Substrate Width, $W_S$ | 30mm |

The beam and sensing capabilities of the microstrip antenna are influenced by its radiation efficiency and gain, where a reduction in efficiency affects directivity and overall gain, impacting signal reflection and transmission. Due to the nature of the rubber material, achieving stable permittivity is crucial for maintaining antenna performance at 5 GHz. Therefore, the antenna has been designed to resonate at 5 GHz, aligning with the Wi-Fi frequency band to ensure compatibility with widely available wireless communication systems while maintaining high efficiency. Several simulations have been carried out to select the best antenna sensor. Ultimately, it was found that the chosen antenna meets all the predefined parameters. During the preliminary study, material variations were tested using a dielectric probe, revealing significant changes in the rubber composition, which align with expected variations in purity and natural quality assessment. These material properties directly influence the antenna's radiation characteristics, highlighting the importance of precise material selection for optimal antenna efficiency.

Besides, the sensor's sensitivity is influenced by the gap between the patch and the feeder, which affects the strength and distribution of the fringing fields [30]. By varying this gap at 1.0mm, 1.5mm, and 2.0mm, the extent of field penetration into the MUT can be controlled, optimizing the sensor's performance for permittivity detection. This principle enables the rectangular microstrip patch antenna sensor to function as a non-destructive dielectric characterization tool, where changes in the resonant frequency shift and return loss, $S_{11}$ provide insights into the dielectric variations of NR materials. Changes in the dielectric properties of the MUT, such as variations in relative permittivity ($\varepsilon_r$), directly influence the electromagnetic wave propagation in the microstrip patch antenna sensor. When the MUT is placed above the antenna, the fringing fields extending beyond the patch interact with it, altering the effective dielectric constant ($\varepsilon_{reff}$) of the system. This results in measurable shifts in the

resonant frequency and return loss, $S_{11}$ of the antenna, which can be analyzed to characterize the dielectric properties of the MUT.

## 3. Results and Discussion

The S-parameter magnitude response shown in Fig. 3 illustrates the resonance behavior of the sensor across a frequency range of 3 to 7 GHz. Fig. 3 depicts the possible impact of Gap Width, G on return loss performance. Specifically, the return loss values for G = 1.0 mm, 1.5 mm, and 2.0 mm are –34 dB, –21 dB, and –15 dB, respectively. It is evident that as Gap Width, G increases from 1mm to 2mm reduces the return loss to approximately -15 dB. The initial dimensions of the antenna were determined based on the calculations presented in [31]. Subsequently, parametric studies and optimization were performed using CST Microwave Studio to enhance the design. The final design was selected when the simulated $S_{11}$ (reflection coefficient) fell below -10 dB at 5 GHz, indicating that less than 10% of the incident power was reflected, while more than 90% was successfully transmitted by the antenna. The graph displays three distinct curves, representing gap sizes of 1.0 mm, 1.5 mm, and 2.0 mm.

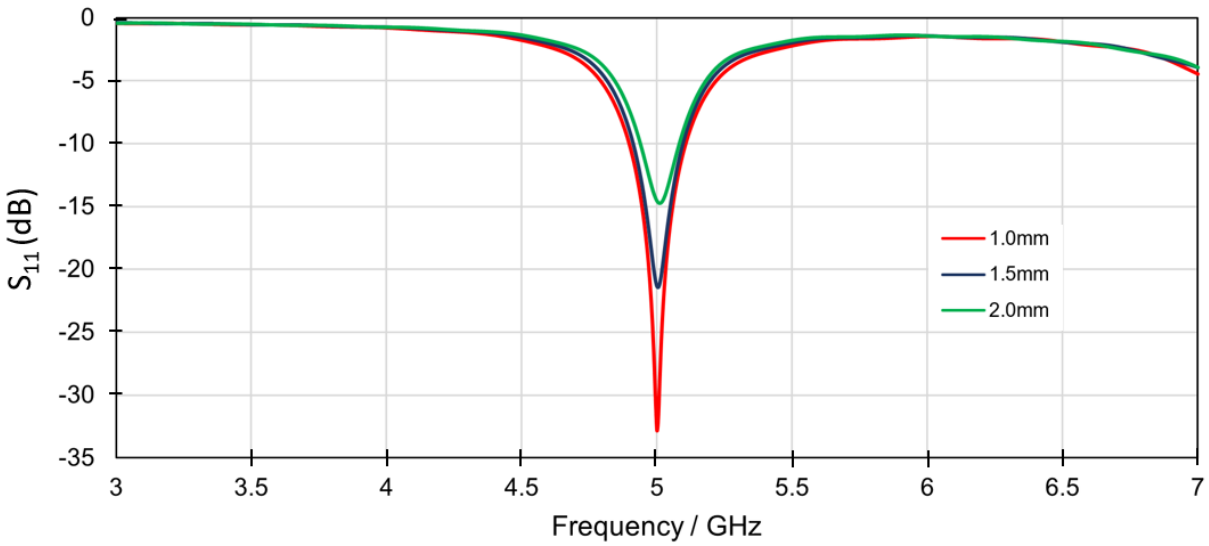


**Fig. 3** *Magnitude of $S_{11}$ for empty MUT*

By defining the quality factor as Q = fr / $\Delta f_{3dB}$ , where fr is the resonance frequency and $\Delta f_{3dB}$ is the 3-dB bandwidth, the sensor demonstrates different Q-factors based on the gap variation. The 1.0 mm gap (red curve) has the deepest and sharpest resonance, corresponding to a larger Q-factor (Q = 345), meaning a more selective and less lossy resonance. As the gap is widened to 1.5 mm (blue curve) and 2.0 mm (green curve), the resonance broadens and becomes shallower, with Q-factors of 102 and 50, respectively. The apparent widening shows a greater level of energy dissipation in addition to reduced field confinement, thereby resulting in higher losses. However, the observed pattern in resonance characteristics shows that adjustment of the gap size not only affects the frequency response and general selectivity of the system but also the sensor's interaction with the surrounding material. A widened resonance enables more effective coupling to external dielectric properties, hence enhancing the sensitivity of the sensor to changes in permittivity and responsiveness to environmental changes.

Fig. 4 illustrates the three-dimensional (3D) radiation pattern of a microstrip patch antenna, indicating its directivity and polarization properties. Red, green, and blue lines indicating the E-plane and H-plane radiation patterns across various orientations confirm the antenna's functionality in more than a single angular direction. Furthermore, the outer three-dimensional surface plot indicates radiation intensity distribution, hence presenting interesting facts about the antenna's efficiency and gain. The radiation pattern indicates that the antenna has a directional radiation characteristic, which consists of a main radiation lobe radiating away from the patch configuration.

Int. Journal of Integrated Engineering Vol. 17 No. 6 (2025) p. 280-291

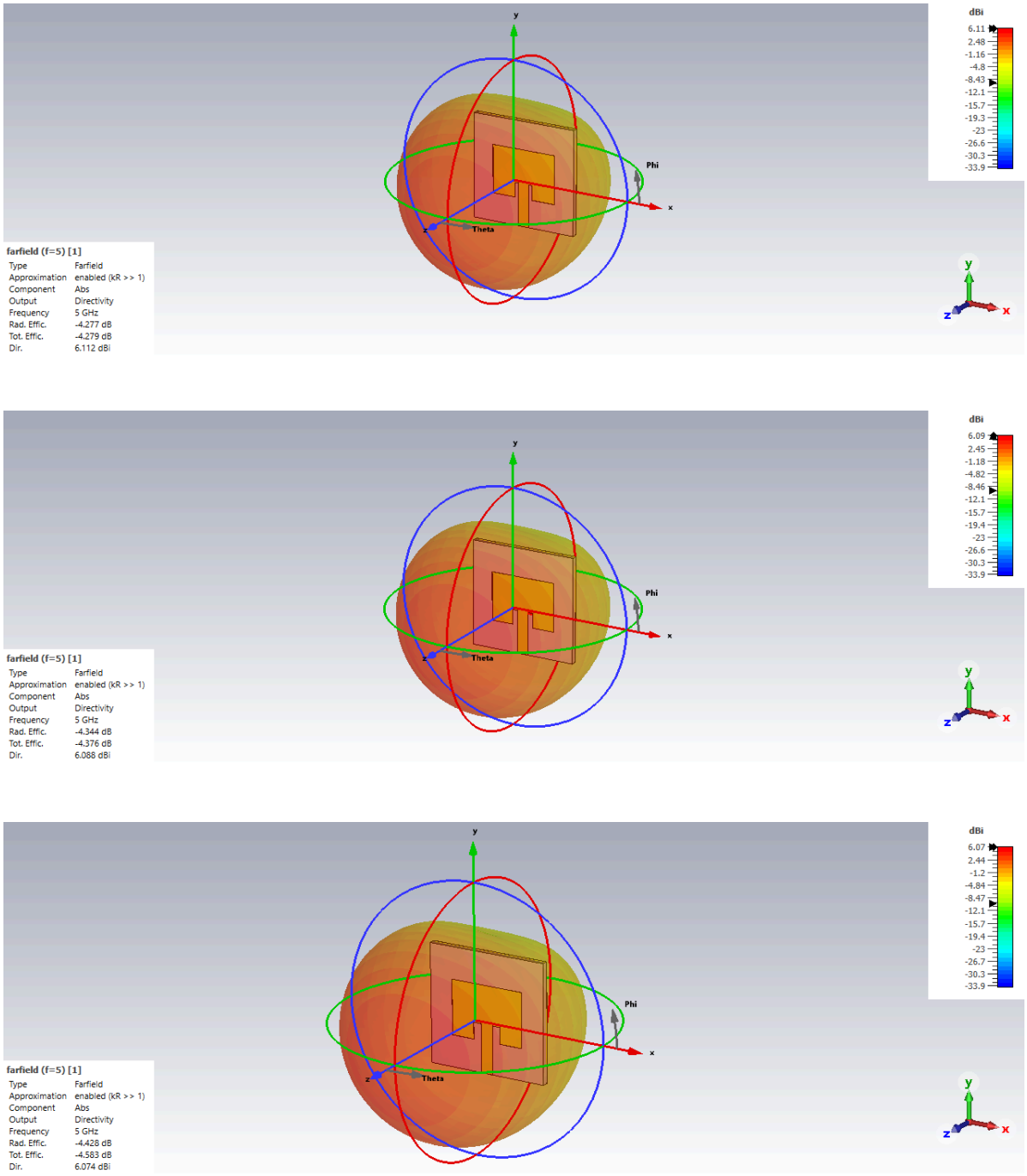


**Fig. 4** *3D radiation pattern of the microstrip patch antenna*

The S-parameter ($S_{11}$) analysis under changing dielectric constants ($\varepsilon_r$) and sensor gaps (air gaps) is shown in Fig. 5. The results show that the dielectric constant ($\varepsilon_r$) and sensor gap both greatly affect the S-parameter ($S_{11}$) response in terms of resonance frequency and return loss. Examination of $S_{11}$ plots for various conditions shows that when the dielectric constant ($\varepsilon_r$) is raised from 2.7 to 4.8, there is a comparatively slight decrease in the resonance frequency. The spacing between the sensor and the substrate also significantly affects resonance behavior. More specifically, if the air gap is 1 mm, then return loss is greater, which is a sign of better resonance and better coupling of energy. As the gap increases to 1.5 mm, the resonance depth is observed to decrease, pointing towards a high level of impedance mismatch. When the spacing is further increased to 2 mm, the resonance frequency undergoes a shift towards a higher level, along with a further decrease in return loss, which implies lesser coupling between the substrate and the sensor.

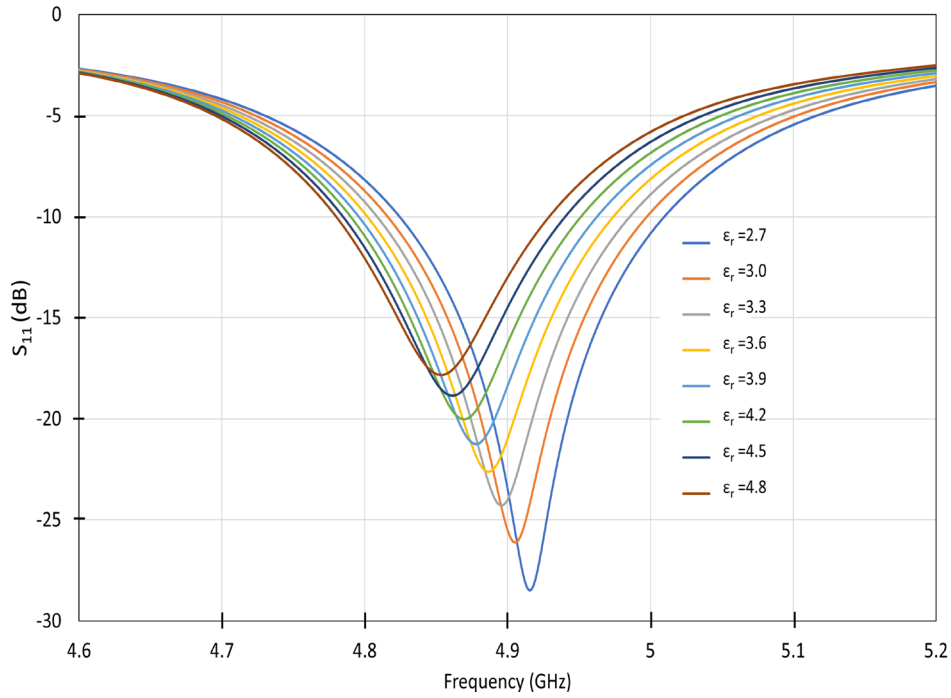
0
-5
-10
-15
-20
-25
-30
S11 (dB)
4.6
4.7
4.8
4.9
5
5.1
5.2
Frequency (GHz)
εr =2.7
εr =3.0
εr =3.3
εr =3.6
εr =3.9
εr =4.2
εr =4.5
εr =4.8

**(a)**

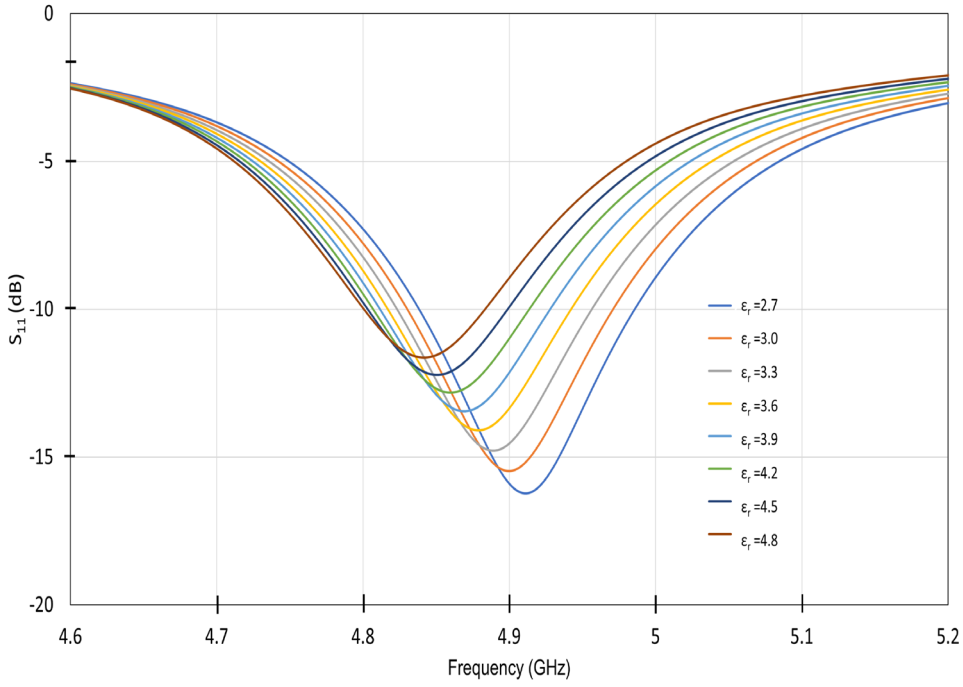
0
-5
-10
-15
-20
S11 (dB)
4.6
4.7
4.8
4.9
5
5.1
5.2
Frequency (GHz)
εr =2.7
εr =3.0
εr =3.3
εr =3.6
εr =3.9
εr =4.2
εr =4.5
εr =4.8

**(b)**

Int. Journal of Integrated Engineering Vol. 17 No. 6 (2025) p. 280-291

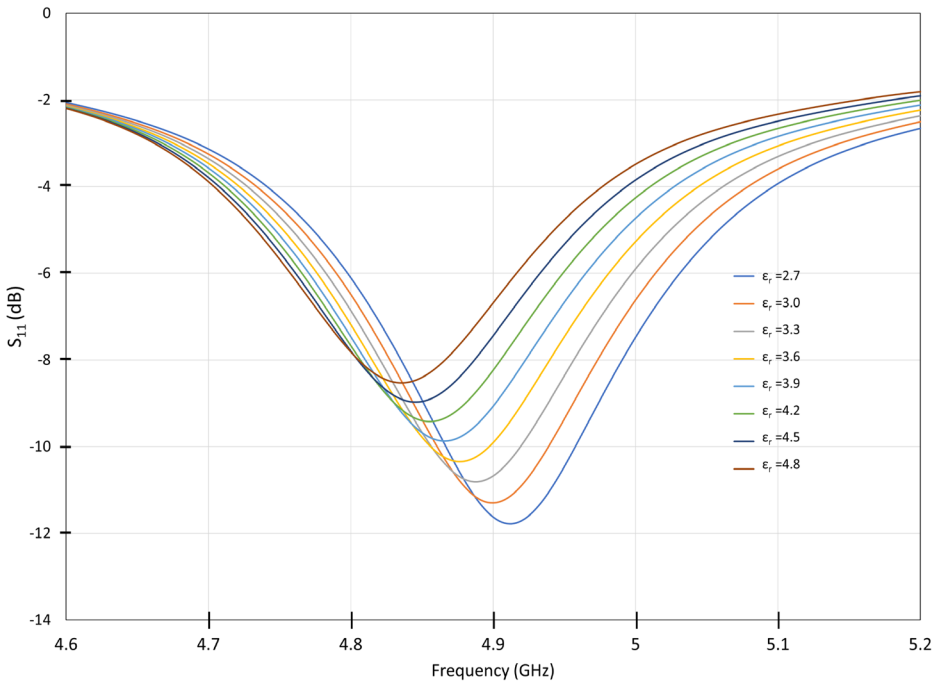


**(c)**

**Fig. 5** *Sensor response for different $\varepsilon_r$ at gap of (a) 1mm; (b) 1.5mm; and (c) 2mm*

Fig. 6 shows the relationship between relative permittivity and normalized resonance frequency for sensor gaps of 1.0 mm, 1.5 mm, and 2.0 mm. The frequency shift results from the antenna's interaction with the Material Under Test (MUT), where higher permittivity leads to lower resonance frequencies due to stronger electromagnetic coupling. This inverse relationship occurs because materials with higher permittivity slow wave propagation. Linear regression ($R^2$ above 0.997) confirms a strong correlation across all gaps, indicating reliable permittivity characterization. However, slope differences highlight the impact of gap size on sensitivity: a 1.0 mm gap shows a steeper slope, indicating higher sensitivity, while a 2.0 mm gap shows a gentler slope and smoother frequency variation. This behaviour is due to changes in field penetration, where smaller gaps confine the field closer to the MUT. Thus, gap size can be tuned to optimize sensor performance for specific applications.

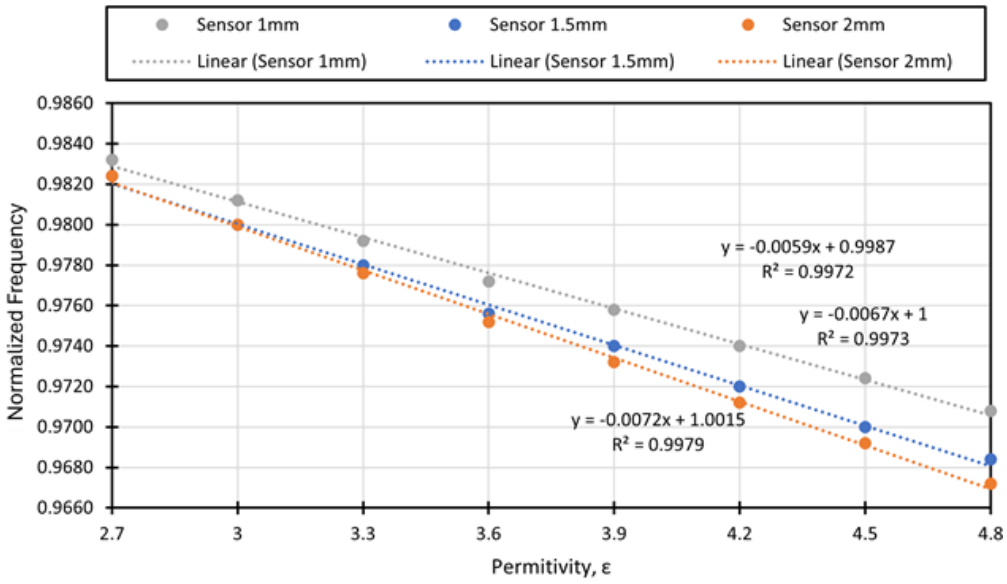


**Fig. 6** *The permittivity $\varepsilon_r$ of the MUT function of the normalized resonance frequency*

## 4. Conclusion

In this study, a compact microstrip patch antenna sensor is presented for permittivity characterization. The sensor, designed at 5 GHz using CST Studio Suite, demonstrates performance that is strongly influenced by critical parameters such as resonant frequency, effective permittivity, Q-factor, and return loss. These parameters directly impact the sensor's sensitivity to changes in the dielectric properties of the Material Under Test (MUT). The results show that when an MUT is placed on the antenna with varying gaps of 1 mm, 1.5 mm, and 2 mm, the antenna maintains a resonant frequency at 5 GHz, with return losses of approximately 15 dB, 22 dB, and 34 dB, respectively. Additionally, as the relative permittivity ($\varepsilon_r$) of the MUT layer is varied from 2.7 to 4.8, a slight shift in the resonance frequency is observed, indicating the antenna's responsiveness to dielectric changes. Among the tested configurations, a 2.0 mm gap between the patch and the MUT yielded the best sensing performance, demonstrating high sensitivity to permittivity variations. Optimizing patch dimensions, substrate properties, and gap spacing ensures accurate and reliable permittivity detection, making the sensor well-suited for dielectric sensing applications.

## Acknowledgement

This research was supported by the Ministry of Higher Education (MOHE) through the Fundamental Research Grant Scheme (FRGS/1/2024/TK07/UTHM/02/7).

## Conflict of Interest

The manuscript has not been published elsewhere and is not under consideration by other journals. All authors have approved the review, agree with its submission and declare no conflict of interest on the manuscript.

## Author Contribution

*The authors confirm contribution to the paper as follows:* ***study conception and design:*** *Muhammad Sazlan Abdul Kadar, Fatin Hamimah Ikhsan, Yee See Khee;* ***data collection:*** *Siti Zarina Mohd Muji, Ariffuddin Joret;* ***analysis and interpretation of results:*** *Muhammad Sazlan Abdul Kadar, Fauziahanim Che Seman;* ***draft manuscript preparation:*** *Muhammad Sazlan Abdul Kadar, Siti Zarina Mohd Muji, Ruzairi Abdul Rahim. All authors reviewed the results and approved the final version of the manuscript.*

## References

[1] S. Bansal and P. Kaur, "A Review on Microstrip Patch Antenna Sensors : Agriculture , Environment , Health Care and IoT Applications 1 Introduction," vol. 23, pp. 149–169, 2024, https://doi.org/10.37394/23204.2024.23.20.

[2] Z. U. Islam, A. Bermak, and B. Wang, "A Review of Microstrip Patch Antenna-Based Passive Sensors," *Sensors*, vol. 24, no. 19, pp. 1–22, 2024, https://doi.org/10.3390/s24196355.

[3] F. H. Ikhsan, S. K. Yee, F. Esa, S. H. Dahlan, V. Nayyeri, and A. Y. I. Ashyap, "Magneto-dielectric properties of Ni0.25Cu0.25Zn0.50Fe2O4–BaTiO3 and its application as substrate of microstrip patch antennas," *J. Mater. Sci. Mater. Electron.*, vol. 34, no. 15, pp. 1–15, 2023, https://doi.org/10.1007/s10854-023-10595-4.

[4] G. Song, B. Zhang, Y. Lyu, T. Sun, X. Wang, and C. He, "Application of frequency doubling in micro-strip patch antenna for wireless strain detection," *Sensors Actuators, A Phys.*, vol. 321, p. 112403, 2021, https://doi.org/10.1016/j.sna.2020.112403.

[5] M. Wang, L. Crocco, M. Li, and M. Cavagnaro, "Slot-Loaded Vivaldi Antenna for Biomedical Microwave Imaging Applications: Influence of Design Parameters on Antenna's Dimensions and Performances," 2024. https://doi.org/10.3390/s24165368.

[6] L. Jin and R. Zhang, "A dual-band wideband high-gain slot loaded microstrip patch antenna," *AEU - Int. J. Electron. Commun.*, vol. 177, p. 155193, 2024, https://doi.org/https://doi.org/10.1016/j.aeue.2024.155193.

[7] K.-D. Jang and J.-H. Lee, "Frequency-Tunable Tri-Band Metamaterial-Inspired Antenna," *IEEE Access*, vol. 13, pp. 21210–21215, 2025, https://doi.org/10.1109/ACCESS.2025.3533023.

[8] J. Yeo and J. I. Lee, "Design of a high-sensitivity microstrip patch sensor antenna loaded with a defected ground structure based on a complementary split ring resonator," *Sensors (Switzerland)*, vol. 20, no. 24, pp. 1–18, 2020, https://doi.org/10.3390/s20247064.

[9] A. Yadegari *et al.*, "Recent advancements in bio-based dielectric and piezoelectric polymers and their biomedical applications," *J. Mater. Chem. B*, vol. 12, no. 22, pp. 5272–5298, 2024,

https://doi.org/10.1039/D4TB00231H.

[10] M. M. Ansari, Y. Heo, K. Do, M. Ghosh, and Y.-O. Son, "Nanocellulose derived from agricultural biowaste by-products–Sustainable synthesis, biocompatibility, biomedical applications, and future perspectives: A review," *Carbohydr. Polym. Technol. Appl.*, vol. 8, p. 100529, 2024, https://doi.org/https://doi.org/10.1016/j.carpta.2024.100529.

[11] M. Vahdatbin, P. Hajikarimi, and E. H. Fini, "Devulcanization of Waste Tire Rubber via Microwave and Biological Methods: A Review," *Polymers (Basel).*, vol. 17, no. 3, pp. 1–30, 2025, https://doi.org/10.3390/polym17030285.

[12] J. Hu, W. Liu, L. Yang, H. Lv, C. Zhan, and P. Qiao, "Research on classification methods for rubber based on terahertz time-domain spectroscopy with data fusion strategy," *Infrared Phys. Technol.*, vol. 139, no. March, p. 105324, 2024, https://doi.org/10.1016/j.infrared.2024.105324.

[13] N. S. Khair, N. A. Talip Yusof, Y. A. Wahab, B. S. Bari, N. I. Ayob, and M. Zolkapli, "Substrate-integrated waveguide (SIW) microwave sensor theory and model in characterising dielectric material: A review," *Sensors Int.*, vol. 4, p. 100244, 2023, https://doi.org/https://doi.org/10.1016/j.sintl.2023.100244.

[14] J. M. Sweety Jaina, Pankaj Kumar Mishra, Vandana Vikas Thakare, "Design and Analysis of Moisture Content of Hevea Latex Rubber Using Microstrip Patch Antenna with DGS," *Mater. Today Proc.*, vol. 29, pp. 556–560, 2020, https://doi.org/10.1016/j.matpr.2020.07.312.

[15] A. F. Ahmad, Z. Abbas, and S. J. Obaiys, "Analysis and Optimal Design of a Microstrip Sensor for Moisture Content in Rubber Latex Measurement," vol. 6, no. 2, pp. 49–62, 2012.

[16] A. B. . Yahaya N.Z., Abbas Z., Ismail M.A., "Determination of Moisture Content of Hevea Rubber Latex Using a Microstrip Patch Antenna," vol. 2, no. 1, pp. 1290–1293, 2012.

[17] Z. Abbas, M. Z. Yahaya, N. Noor, A. Nik, and A. Razak, "Development of Calibration Equation Based on Complex Permittivity of Hevea Development of Calibration Equation Based on Complex Permittivity of Hevea Rubber Latex," no. July, 2015.

[18] A. Nuan-On and N. P. and C. S. , Niwat Angkawisittpan, "Design and Fabrication of Modified SMA-Connector Sensor for Detecting Water Adulteration in Honey and Natural Latex," *Appl. Syst. Innov.*, 2021, https://doi.org/https://doi.org/ 10.3390/asi5010004.

[19] L. G. Ayalew and F. M. Asmare, "Design and optimization of pi-slotted dual-band rectangular microstrip patch antenna using surface response methodology for 5G applications," *Heliyon*, vol. 8, no. 12, p. e12030, 2022, https://doi.org/10.1016/j.heliyon.2022.e12030.

[20] M. T. Islam *et al.*, "Design of a microstrip patch antenna for the Ku band applications," *Mater. Today Proc.*, vol. 42, pp. 1502–1505, 2020, https://doi.org/10.1016/j.matpr.2021.01.445.

[21] C.A. Balanis, *Antenna theory: Analysis and Design, 4th edn. (Wiley, Hoboken, 2016)*.

[22] M. S. H. Firaj, Md. Rashedin, "Designing a High Gain Rectangular Microstrip Patch Antenna Working at 3 GHz for RADAR," *Int. J. Innov. Sci. Res. Technol.*, vol. 9, no. 4, pp. 1967–1971, 2024, https://doi.org/10.38124/ijisrt/IJISRT24APR1771 II.

[23] M. A. Saeed and A. O. Nwajana, "A review of beamforming microstrip patch antenna array for future 5G / 6G networks," *Front. Mech. Eng.*, no. February, pp. 1–15, 2024, https://doi.org/10.3389/fmech.2023.1288171.

[24] B. Bariser, I. Umakoglu, M. Namdar, and A. Basgumus, "Microstrip Patch Antenna Design for 5G and Beyond Wireless Communication Systems," *J. Sci. Reports-A*, vol. 0, no. 274, pp. 83–98, 2024, https://doi.org/10.59313/jsr-a.1518956.

[25] R. K. V. and V. S. Brijesh Mishra, Aditya Kumar Singh, T Y Satheesha, "From Past to Present: A Comprehensive Review of Antenna Technology in Modern Wireless Communication," *J. Eng. Sci. Technol. Rev.*, vol. 17, no. 3, pp. 179–200, 2024, https://doi.org/10.25103/jestr.173.20.

[26] P. A. M. Mercy, "Novel nanocomposite based microstrip patch antenna for C and X band applications," *Mater. Chem. Phys.*, vol. 326, p. 129593, 2024, https://doi.org/https://doi.org/10.1016/j.matchemphys.2024.129593.

[27] H. Abudrbala, "Design and Simulation of a 3 GHz Rectangular Microstrip Patch Antenna Using ADS," *Sebha Univ. J. Pure Appl. Sci.*, no. October, 2025, https://doi.org/10.51984/JOPAS.V24I3.3646.

[28] K. Singh, M. Dhayal, and S. Dwivedi, "Design and analysis of ultra - wideband microstrip patch antenna with various conductive materials for terahertz gap," *Discov. Appl. Sci.*, 2024, https://doi.org/10.1007/s42452-024-05886-2.

[29] A. S. A. Gaid *et al.*, "Design and analysis of a low profile , high gain rectangular microstrip patch antenna for 28 GHz applications," *Cogent Eng.*, vol. 11, no. 1, p., 2024, https://doi.org/10.1080/23311916.2024.2322827.

[30] M. Shaban, "Design and Modeling of a Reconfigurable Multiple Input, Multiple Output Antenna for 24 GHz Radar Sensors," 2025. https://doi.org/10.3390/modelling6010002.

[31] İ. Umakoğlu, B. Barışer, M. Namdar, and A. Başgümüş, "Microstrip Patch Antenna Design for 5G and Beyond Wireless Communication Systems," *J. Sci. Reports-A*, no. 058, pp. 83–98, 2024, https://doi.org/10.59313/jsr-a.1518956.